ARTICLE

Resonance Raman Study of Aggregated *Meso*-tetra(4-pyridinium)porphyrin Diacid

Zun-yun Li, Tong-tong Lu, Tian-jing He, Fan-chen Liu, Dong-ming Chen*

Department of Chemical Physics, University of Science and Technology of China, Hefei 230026, China

(Dated: Received on June 4, 2009; Accepted on June 19, 2009)

Resonance Raman spectra of aggregated *meso*-tetra(4-pyridinium)porphyrin diacid (H_8TPyP^{6+}) were studied with excitation near the exciton absorption bands of 470 nm. The UV-Vis absorption and resonance light scattering spectra of H_8TPyP^{6+} monomers and aggregates were also measured. The observed Raman bands of monomeric and aggregated H_8TPyP^{6+} were assigned on the basis of the observed deuteration shifts and by comparing with the Raman spectra of analogous porphyrin diacids. Aggregation causes moderate downshifts (2−6 cm^{-1}) for high-frequency modes involving the in-plane CC/CN stretches of the porphyrin core and a dramatic upshift (12 cm^{-1}) for the out-of-plane saddling mode of the porphyrin ring. The structural changes induced by aggregation and the possible hydrogen bonding interaction between the H_8TPyP^{6+} molecules in the aggregate are discussed based on the spectral observations.

Key words: Porphyrin diacid, Aggregate, Resonance Raman, Molecular vibration

I. INTRODUCTION

Molecular aggregates of porphyrin-related macrocycles are of interest because of their structural resemblance to the light-harvesting pigments of the natural photosynthesis systems and their remarkable nonlinear optical properties [1−6]. It has been found that some water-soluble porphyrins with tetraaryl-substitutents tend to self-assemble into aggregates by controlling the concentration, pH, ionic strength, and temperature [7−24]. Among these synthetic porphyrins, tetra(4-sulfonatophenyl)porphyrin diacid ($H_4TPPS_4{}^{2-}$) aggregates have been most extensively studied [7−16]. Spectroscopic evidence demonstrated that the $H_4TPPS_4{}^{2-}$ aggregates form a high-ordered one-dimensional linear chain [10,13−16]. The atomic force microscope (AFM) study indicated that the $H_4TPPS_4{}^{2-}$ aggregates have ring-shaped structures stacking into flattened nanotubes on silicon substrates [12]. Resonance Raman scattering (RRS) has been demonstrated to be a valuable tool to study the structures and interactions of the porphyrin aggregates [13−19]. By using excitation near the exciton band, the RRS of aggregated $H_4TPPS_4{}^{2-}$ has been reported by several groups to reveal the intra-/inter-molecular structures and excitonic coupling [14−16]. The Raman spectra of other *meso*-sulfonatophenyl substituted porphyrins ($TPPS_n$, n=1, 2, 3) have been measured to obtain the information about the influences of peripheral groups on the structures of the porphyrin molecules and their aggregates [17]. Choi *et al.* has used resonance Raman (RR) technique to study the counterion-dependent structure and excitonic coupling in the aggregates of *meso*-tetra(4-carboxylphenyl)porphyrin (TCPP) diacid [19]. The structure of porphyrin J-aggregates have also been studied by vibrationally and electronically doubly resonant sum frequency generation (SFG) spectroscopy [24].

Meso-tetra(4-pyridyl)porphyrin (TPyP) is an important porphyrin derivative with wide applications. In weak acidic aqueous solution, the nitrogen atoms on the pyridyl groups of the neutral free base H_2TPyP can combine with protons to form tetra-protonated tetra(4-pyridinium)porphyrin free base (H_6TPyP^{4+}). With increasing the acidity, the central pyrrole nitrogen atoms can combine with two additional hydrogen atoms to form the fully N-protonated porphyrin diacid H_8TPyP^{6+} (structure shown in Fig.1). Recently, Luca *et al.* showed that large aggregates of TPyP were formed in the dichloromethane solutions in the presence of organic or inorganic acids [22]. The protonated species and their aggregation behavior were found depending on the nature of the counteranions. A central-to-edge packing model has been proposed for the aggregates, in which the intermolecular hydrogen bonds mediated by the halide counter anions were thought to play an important role in the stabilization of the aggregates [22].

In this work, we report the Raman spectra of monomeric and aggregated porphyrin diacid H_8TPyP^{6+} (denoted as m-H_8TPyP^{6+} and agg-H_8TPyP^{6+}, respectively) and their deuterated derivatives. The observed

*Author to whom correspondence should be addressed. E-mail: dmchen@ustc.edu.cn, Tel: +86-551-3606145

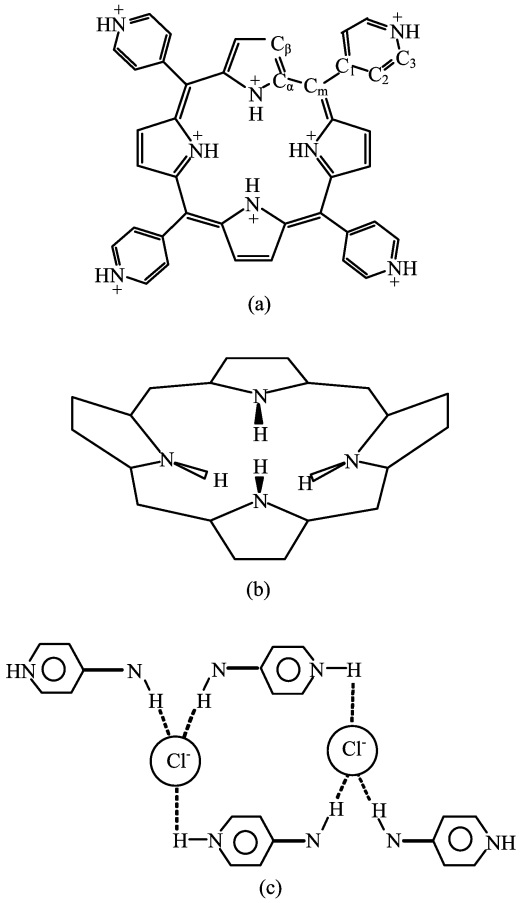

FIG. 1 Structure sketches of (a) H_8TPyP^{6+} with the labels of the atoms, (b) the saddling distortion for the core of a porphyrin diacid, and (c) the Cl^- mediated hydrogen bonding model for the H_8TPyP^{6+} aggregate [22].

Raman bands were assigned on the basis of the deuteration shifts and by comparing with the analogous systems [25−27]. The possible associating manner of the H_8TPyP^{6+} molecules in the aggregate is discussed based on the spectral observations.

II. EXPERIMENTAL METHOD

The *meso*-tetra(4-pyridyl)porphyrin was purchased from Aldrich Chemical Co. and used as received. To prepare the solution of monomeric diacid H_8TPyP^{6+}, the solid powder (5 mg) of the free-base *meso*-tetra(4-pyridyl)porphyrin (H_2TPyP) was dissolved in 5 mL dilute HCl acid (∼1 mol/L). Its N-deuterated analogue (D_8TPyP^{6+}) was prepared with similar method except that the DCl acid (∼1 mol/L in D_2O) was used as the solvent. The agg-H_8TPyP^{6+} and its deuterated analogue (agg-D_8TPyP^{6+}) were synthesized following procedures similar to those reported in Ref.[22]. For agg-H_8TPyP^{6+}, 2 mg of H_2TPyP powder were firstly dissolved in 20 mL of dichloromethane, then a small amount (∼10 μL) of concentrated hydrochloric acid was injected into the solution with a miniliter syringe. The solution was shaken gently to uniformity. The agg-D_8TPyP^{6+} solutions were prepared with a similar method, except that the acidification of solutions was carried out with DCl acid (25% in D_2O). The concentrations of TPyP were adapted to ∼3.8 μmol/L for the UV-Vis absorption and the resonance light scattering (RLS) measurements. For Raman experiments, the concentrations of TPyP are 0.2 mmol/L (m-H_8TPyP^{6+} and m-D_8TPyP^{6+}), 0.06 mmol/L (agg-H_8TPyP^{6+}), and 0.03 mol/L (agg-D_8TPyP^{6+}).

The UV-Vis absorption spectra were measured in a 10 mm quartz cell at room temperature using a Shimadu UV-2401PC spectrometer. The RLS spectra were recorded on a LS55 spectrofluorimeter with a quartz fluorescence cell. The RLS spectra were obtained by synchronously scanning the excitation and emission wavelengths to generate an excitation profile for the elastically scattered light. The solution Raman spectra were measured on a Labram-010 Raman spectrometer. A lens with 40 mm focal distance was used to focus the incident laser beam and collect the scattering light with a back-scattering geometry. The 488 nm line of an Ar^+ laser (Spectra-Physics 163-C12) was used as the excitation source with the power of 5 mW on samples. The time constant of the air-cooled CCD detector was 50 seconds, and 4 scans were accumulated for each Raman spectrum.

III. RESULTS AND DISCUSSION

A. The UV-Vis and RLS characterization of H_8TPyP^{6+} aggregation

It is known that the UV-Vis absorptions of a porphyrin compound are due to the electronic transitions from the ground state (S_0) to the two lowest singlet excited states S_1 and S_2 [28]. The $S_0 \rightarrow S_1$ transition gives rise to the weak Q bands in visible region while $S_0 \rightarrow S_2$ transition produces a strong B band in the near UV region. Figure 2 displays the UV-Vis absorption spectra of TPyP at different conditions. In neutral dichloromethane solution (Fig.2(a)), the spectrum shows the typical features of a free-base porphyrin, consisting of an intense B band (Soret band) at 416 nm and four weak Q bands at 512, 545, 588, and 644 nm. In hydrochloric acid aqueous solution, the absorption bands shift to 443 (B band), 590 and 640 nm (Q bands), indicating the formation of N-protonated diacid in the monomer form (m-H_8TPyP^{6+}). The reduced Q bands in H_8TPyP^{6+} as compared with the free base is attributed to the existence of 4-fold rotary-reflection axis for the diacid. In the dichloromethane solution with a small amount of concentrated hydrochloric acid, the absorption bands shift to 470 (B band), 614 and 667 nm (Q bands), due to the formation of the aggregated porphyrin diacid (agg-H_8TPyP^{6+}). The dramatic redshift of agg-H_8TPyP^{6+} as compared with m-H_8TPyP^{6+} is

DOI:10.1088/1674-0068/22/04/346-352

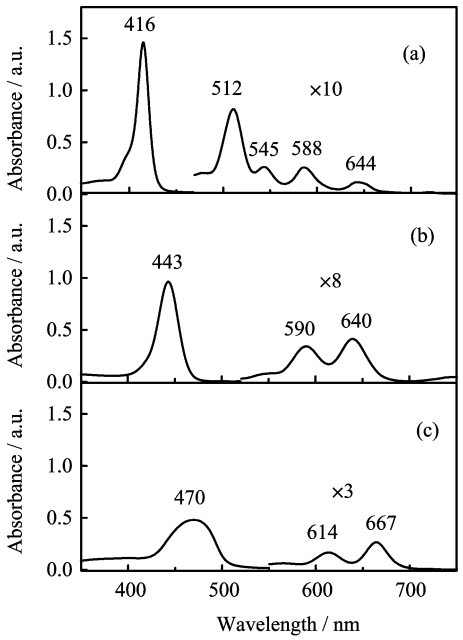

FIG. 2 The UV-Vis absorption spectra of (a) H_2TPyP in pure CH_2Cl_2, (b) m-H_8TPyP^{6+} in 1 mol/L aqueous HCl solution, and (c) agg-H_8TPyP^{6+} in CH_2Cl_2/HCl.

attributed to the exciton coupling in the aggregates [21,22]. The Soret band was broadened at the expense of decreasing of peak intensity, which may be attributed either to the increased distortion of porphyrin macrocycle or to the formation of extended aggregates.

The RLS has proven to be a powerful tool to study the aggregation and association of molecules in solutions [29−32]. For the porphyrin aggregates, the existence of an excitonically coupled (delocalized) electronic transition is characterized by strong RLS signals that are slightly red-shifted from the corresponding absorption band [7,22,30]. In contrast, the RLS signals are usually weak when the molecules in the solution exist as monomers. The RLS of H_2TPyP, m-H_8TPyP^{6+}, and agg-H_8TPyP^{6+} are shown in Fig.3. Both the free base H_2TPyP in neutral CH_2Cl_2 solution and the H_8TPyP^{6+} in HCl aqueous solution exhibit rather weak light scattering profiles, reflecting that the porphyrin molecules in these two samples exist as monomeric form. The H_8TPyP^{6+} in CH_2Cl_2/HCl solution displays a very intense peak at 505 nm in the RLS spectra, indicating that the measured species exist as aggregates. The observed UV-Vis and RLS spectra are well consistent with those reported in Ref.[22].

B. Raman spectra of H_8TPyP^{6+}

1. Experimental results

Figure 4 displays the measured Raman spectra of m-H_8TPyP^{6+} and m-D_8TPyP^{6+} in HCl/DCl aqueous solutions. The Raman spectra of agg-H_8TPyP^{6+} and

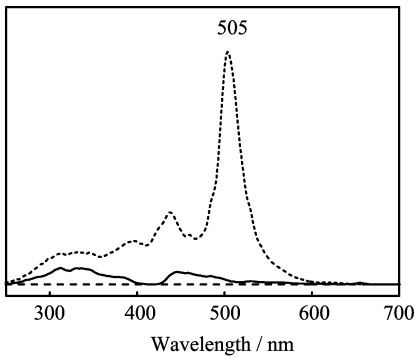

FIG. 3 The RLS spectra of H_2TPyP in CH_2Cl_2 (solid line), m-H_8TPyP^{6+} in 1 mol/L HCl aqueous solution (dashed line), and agg-H_8TPyP^{6+} in CH_2Cl_2/HCl (short-dashed line).

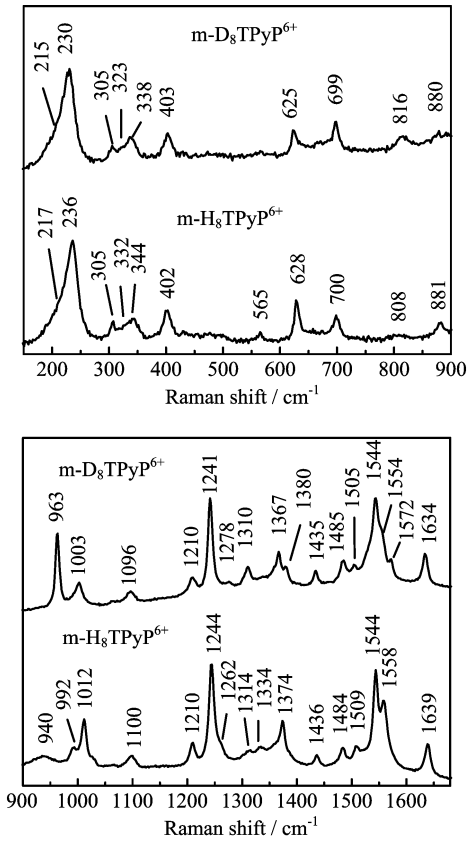

FIG. 4 Solution Raman spectrum of m-H_8TPyP^{6+} and m-D_8TPyP^{6+} in 1 mol/L HCl/DCl. Excitation wavelength: 488 nm.

agg-D_8TPyP^{6+} in CH_2Cl_2/HCl(DCl) solution are displayed in Fig.5, where the Raman signals due to the solvent (CH_2Cl_2) were marked with "s". The excitation wavelength (488 nm) is quite close to the B band of the monomer and the J_B band of the aggregate, which favors Franck-Condon mechanism (Albrecht's A-term mechanism) of resonance Raman enhancement [33,34]. Table I shows the observed Raman frequencies and their

DOI:10.1088/1674-0068/22/04/346-352

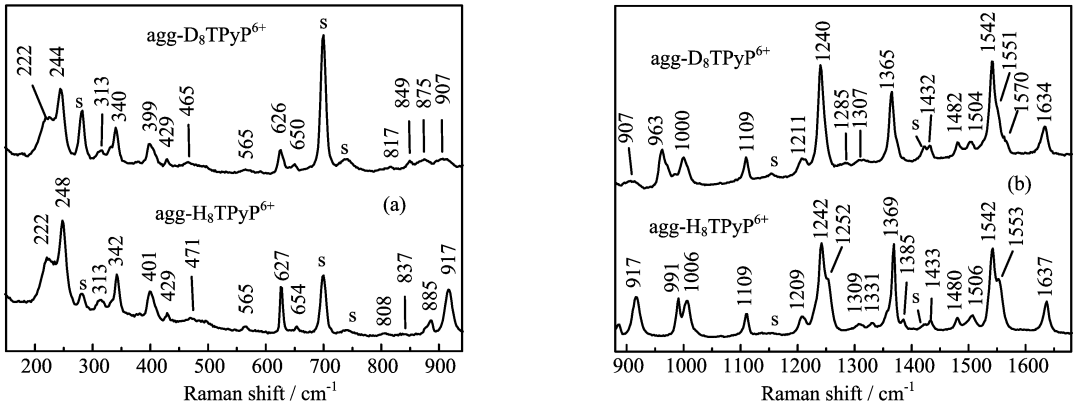

FIG. 5 Solution Raman spectra of agg-H_8TPyP^{6+} and agg-D_8TPyP^{6+} in CH_2Cl_2 (with HCl/DCl). Excitation wavelength: 488 nm. s bands show the solvent bands.

assignments, where the mode numbers and the corresponding local coordinates of skeletal modes follow those used in analogous porphyrin compounds [25−27].

Unlike most of the normal metalloporphyrins those have the porphyrin ring of D_{4h} effective symmetry, the four pyrrole rings in the porphyrin diacids are tilted alternately from the mean-plane of the porphyrin ring due to the steric hindrance of the central hydrogen atoms, forming a core structure of effective D_{2d} symmetry [25]. In addition, the structure of H_8TPyP^{6+} molecule in the aggregate is expected to be lower compared with H_8TPyP^{6+} monomer due to the packing effect. Despite this, we classify the molecular vibrations of agg-H_8TPyP^{6+} according to D_{2d} point group for simplicity.

2. $C_\beta-C_\beta$ and $C_\alpha-C_m$ stretching modes

The molecular vibrations of *meso*-tetraphenylporphyrin diacid (H_4TPP^{2+}) have been studied in detail by isotopic labeling and density function theory (DFT) calculation [25], providing useful references for the vibrational analysis of H_8TPyP^{6+}. Due to the relatively large force constants, the stretching vibrations of the $C_\beta-C_\beta$ and $C_\alpha-C_m$ bonds are usually in 1450−1650 cm^{-1} [16,25-27]. In this region, five RR band were observed at 1637, 1553, 1542, 1506, and 1480 cm^{-1} for agg-H_8TPyP^{6+}. In m-H_8TPyP^{6+}, the corresponding bands were measured at 1639, 1558, 1544, 1509, and 1484 cm^{-1}. By comparison with the corresponding modes of H_4TPP^{2+}, the 1553, 1542, and 1480 cm^{-1} bands of agg-H_8TPyP^{6+} are assigned to asymmetric $C_\alpha-C_m$ stretch ν_{10} (B_1), $C_\beta-C_\beta$ stretch ν_2 (A_1), and $C_\beta-C_\beta$ stretch ν_{11} (B_1), respectively. The deuteration shifts for these bands are small, reflecting the fact that $C_\beta-C_\beta$ and $C_\alpha-C_m$ stretching vibrations do not severely interact with the motions of other atoms in porphyrin ring [27]. The 1637 and 1506 cm^{-1} bands of agg-H_8TPyP^{6+} can be assigned to the pyridinium CC/CN stretching modes. These two bands show 2−3 cm^{-1} downshift upon D_8 substitution, indicating a weak coupling of CC/CN stretching with NH/ND bending of the pyridinium groups. In H_4TPP^{2+}, the corresponding phenyl C−C stretch mode has been observed at 1597/1494 cm^{-1} in the Raman spectrum [25].

3. RR bands in the region 900−1450 cm^{-1}

Since the $C_\alpha-C_\beta$ and $C_\alpha-N$ stretching motions in the porphyrin are strongly mixed with each other, the vibrations involving $C_\alpha-C_\beta$ and $C_\alpha-N$ stretches are better described as pyrrole half-ring ν(Pyr/2), quarter-ring stretching ν(Pyr/4) and pyrrole breathing ν(Pyr. br.) modes [26]. Vibrational bands in the 1300−1450 cm^{-1} region are most likely from the pyrrole quarter-ring and symmetric half-ring stretches. By comparing with H_4TPP^{2+}, we assign the 1433, 1369, and 1309 cm^{-1} bands of agg-H_8TPyP^{6+} to the symmetric $C_\alpha-C_m$ stretch ν_3 (A_1), the symmetric half-ring ν_4 (A_1), and quarter-ring stretch ν_{12} (B_1), respectively. These three bands show deuterate shifts by 1, 4, and 2 cm^{-1}, respectively. In m-H_8TPyP^{6+}, ν_3, ν_4, and ν_{12} were observed at 1436, 1374, and 1314 cm^{-1}, respectively, and their D_8 shifts are 1, 7, and 4 cm^{-1}, respectively. The ν_3 and ν_4 modes of agg-H_8TPyP^{6+} decreased by 3 and 5 cm^{-1}, respectively, compared with m-H_8TPyP^{6+}, suggesting a small in-plane distortion of pyrrole rings in the aggregated H_8TPyP^{6+}. The weak band at 1331 cm^{-1} in agg-H_8TPyP^{6+} and the one at 1334 cm^{-1} in m-H_8TPyP^{6+} are tentatively assigned to the in-plane N−H rocking of the pyrrole rings.

We assign the strong 1242 cm^{-1} band of agg-H_8TPyP^{6+} and the 1244 cm^{-1} band of m-H_8TPyP^{6+} to the C_m-Py stretch (ν_1). For the *meso*-aryl substituted porphyrins, ν_1 mode usually shows considerable intensity with near B band excitation [26,27]. The ν_1 mode (C_m-Ph stretch) of H_4TPP^{2+} was observed at 1235 cm^{-1} [25], which is close to the corresponding band of H_8TPyP^{6+}. The 1006 and 991 cm^{-1} bands of agg-H_8TPyP^{6+} and their counterparts in m-H_8TPyP^{6+} (1012 and 992 cm^{-1} bands) can be assigned to the pyr-

DOI:10.1088/1674-0068/22/04/346-352

TABLE I Observed Raman frequencies (in cm^{-1}) of m-H_8TPyP^{6+} and agg-H_8TPyP^{6+} as well as their N-D_8 substituted derivatives.

m-H_8TPyP^{6+}	m-D_8TPyP^{6+}	agg-H_8TPyP^{6+}	agg-D_8TPyP^{6+}	ν_i[a]	Assignment[a]
1639	1634	1637	1634		Py ν(CN/CC)
	1572		1570		Py ν(CC)
1558	1554	1553	1551	ν_{10}	$\nu(C_\alpha-C_m)_{as}$
1544	1544	1542	1542	ν_2	$\nu(C_\beta-C_\beta)$
1509	1505	1506	1504		Py ν(CC/CN)
1484	1485	1480	1482	ν_{11}	$\nu(C_\beta-C_\beta)$
1436	1435	1433	1432	ν_3	$\nu(C_\alpha-C_m)_s$
	1380	1385			
1374	1367	1369	1365	ν_4	$\nu(Pyr/2)_s$
1334		1331			Pyr δN−H
1314	1310	1309	1307	ν_{12}	ν(Pyr/4)
1262		1252			
	1278		1285		
1244	1241	1242	1240	ν_1	$\nu(C_m-Py)$
1210	1210	1209	1211		
1100	1096	1109	1109	ν_9	$\delta(C_\beta-H)_s$
1012	1003	1006	1000	ν_{15}	ν(Pyr br)
992	963	991	963	ν_6	ν(Pyr br)
940		917	907		
881	880	885	875	ν_7	$\delta(Pyr\ def)_s$
		837	849		
808	816	808	817		
700	699	–[b]	–[b]	γ_5	$\gamma(Pyr\ fold)_s$
		654	650		
628	625	627	626	γ_{15}	$\gamma(Pyr\ fold)_s$
565		565	565	γ_7	$\gamma(C_\alpha-C_m)$
		471	465		
		429	429		
402	403	401	399	ν_{33}	δ(Pyr rot)
344	338	342	340	ν_8	ν(Pyr transl)
332	323	313	313	γ_{12}	γ(Pyr swivel)
305	305			γ_2	γ(Pyr swivel)
236	230	248	244	γ_{16}	γ(Pyr tilt)
217	215	222	222		Py (oop)

[a] Mode numbering and local coordinate description according to [27]. Py=pyridinium, Pyr=pyrrole.
[b] Masked by a solvent (CH_2Cl_2) band.

role breathing vibrations ν_{15} and ν_6. These two bands show rather large downshifts upon N-D_8 substitution. In addition, for both agg-H_8TPyP^{6+} and m-H_8TPyP^{6+} the intensities of ν_6 increase obviously with N-D_8 substitution, implying that the pyrrole breathing has remarkable interaction with the motion of the N−H(N−D) bonds.

4. RR bands in the region 150−900 cm^{-1}

In the region of 150−900 cm^{-1}, Raman bands were observed at 885, 654, 627, 565, 429, 401, 342, 313, 248, and 222 cm^{-1} for agg-H_8TPyP^{6+} (Fig.5). For m-H_8TPyP^{6+}, evident Raman bands were measured at 881, 700, 628, 402, 344, 332 (shoulder), 305, and 236 cm^{-1} (broad). The 700 cm^{-1} band of m-H_8TPyP^{6+} was not distinguished in agg-H_8TPyP^{6+} due to the coincident band of a strong solvent (CH_2Cl_2) band at this position.

The strong 342 cm^{-1} band of the aggregate and the 344 cm^{-1} band of the monomer are assigned to ν_8 (A_1), the pyrrole translational mode. For a porphyrin compound with planar porphyrin ring (D_{4h} or D_{2h} symme-

DOI:10.1088/1674-0068/22/04/346-352

try), the ν_8 mode is the sole low-frequency vibration expected to exhibit strong enhancement with near B-band excitation [18,26,27]. For the porphyrin diacids, ν_8 mode remains as one of the strongest low-frequency bands, although it is less dominant in intensity due to the out-of-plane (oop) distortion of the porphyrin core. In H_4TPP^{2+}, ν_8 was observed at 335 cm^{-1}, which is close to the frequency (342 cm^{-1}) of the corresponding mode in agg-H_8TPyP^{6+}.

The strong low frequency band of m-H_8TPyP^{6+} at 236 cm^{-1} shows an asymmetric shape and is obviously broadened compared with other bands. Deconvolution of the envelope results in a strong band at 236 cm^{-1} and a weak band at about 217 cm^{-1}. In agg-H_8TPyP^{6+}, two distinct bands were observed at 248 and 222 cm^{-1}. Upon N-D_8 substitutions, the 248 cm^{-1} band of agg-H_8TPyP^{6+} shows 4 cm^{-1} downshift while its 222 cm^{-1} band is almost unchanged. In the 488 nm excited Raman spectrum of H_4TPP^{2+}, analogous bands were observed at 223 and 201 cm^{-1} and were assigned to the oop folding mode γ_{16} (A_1 symmetry under D_{2d}) and phenyl oop deformation, respectively. By comparing with H_4TPP^{2+}, we assign the 248 cm^{-1} band of agg-H_8TPyP^{6+} as well as the 236 cm^{-1} band of m-H_8TPP^{6+} to the porphyrin oop saddling mode γ_{16}, in which the four pyrrole rings tilt around their $C_\alpha-C_\alpha$ axes [27]. As an oop mode, the intensity of γ_{16} in m-H_8TPyP^{6+} and agg-H_8TPyP^{6+} is unusual, since only in-plane modes are expected to be resonantly enhanced with π-π^* excitation [33]. The strong intensity of the oop mode γ_{16} in the diacid was attributable to the symmetry lowering from D_{4h} to D_{2h} in porphyrin diacids [25]. When the effective symmetry of the porphyrin core reduces from the D_{4h} point group to D_{2h}, the oop γ_{16} mode changes from the non-totally symmetric B_{1u} representation of D_{4h} to the totally symmetric A_1 representation of D_{2d}, and therefore can be resonantly enhanced via Franck-Condon mechanism.

C. Discussion

Luca *et al.* have proposed a central-to-edge packing model for the H_8TPyP^{6+} aggregates and suggested that a network of hydrogen bonds plays a critical role in the intermolecular association of the aggregate, although the electrostatic ion pairing and π-stacking interactions also contribute to the stabilization of overall structure of the aggregate [22]. In this model, the halide counter anions participate in the hydrogen bonding by connecting the hydrogen atoms on the pyrrole nitrogen of an H_8TPyP^{6+} molecule with the hydrogen atom on the pyridinium group of an adjacent H_8TPyP^{6+} molecule. The frequency differences between the aggregated and monomeric H_8TPyP^{6+} reflect their differences in the ground state structures. Shelnutt *et al.* have studied the RR spectra of several non-planar metalloporphyrins [35]. It is noticed that the frequency decrease of the in-plane CC/CN stretching modes ν_2, ν_{10}, ν_{11}, ν_4, and ν_{19} can correlate with the prolonging of the CC/CN bonds of these porphyrin compounds [35]. Compared with m-H_8TPyP^{6+}, the frequencies of ν_2, ν_{10}, ν_{11}, ν_4, and ν_{15} modes of agg-H_8TPyP^{6+} decrease by 2−6 cm^{-1}, which implies a prolonging of the porphyrin CC/CN bonds in the aggregates as compared with the monomers. In addition, the oop porphyrin saddling mode at 236 cm^{-1} (γ_{16}) in m-H_8TPyP^{6+} upward shifts to 248 cm^{-1} in agg-H_8TPyP^{6+}. We attribute this dramatic upward shift of the γ_{16} mode in the aggregates to the Cl^- mediated hydrogen bonding between the adjacent H_8TPyP^{6+} molecules. The existence of $N-H\cdots Cl$ hydrogen bond exerts a strong constraint for the oop tilt of the pyrrole ring and thus enhances the restore force, causing the frequency of the γ_{16} mode to upward shift dramatically. It was also noticed that most of the strong RR bands in agg-H_8TPyP^{6+} show smaller N-D_8 shifts as compared with their counterparts in m-H_8TPyP^{6+}, which provides further evidence for the existence of hydrogen bonds in the aggregate.

IV. CONCLUSION

We measured the Raman spectra of monomeric and aggregated tetra(4-pyridinium)porphyrin diacid (H_8TPyP^{6+}) excited at 488 nm, near resonant with the B band of monomer and the J_B exciton band of the aggregate. UV-Vis absorption and RLS spectra were used to characterize the aggregation states of the studied systems. The RR spectra of the deuterated monomers and aggregates were also recorded, and the assignments of observed Raman bands of H_8TPyP^{6+} were proposed on the basis of the deuteration shifts and by comparing with their well-studied structural analog H_4TPP^{2+}. The RR spectrum of the aggregated H_8TPyP^{6+} was found to exhibit clear and characteristic changes compared with the monomers, and the structural and interaction implications of the aggregates were discussed based on the spectral observations. It was considered that the dramatic upshift of the out-of-plane porphyrin saddling mode (γ_{16}) in the aggregates can be attributed to the Cl^- mediated hydrogen bonding between the adjacent H_8TPyP^{6+} molecules. Our spectral observations are consistent with the slide face-to-face model and the hydrogen bonding driven mechanism for the H_8TPyP^{6+} aggregates proposed by Luca *et al.* [22].

V. ACKNOWLEDGMENTS

This work was supported by the National Natural Science Foundation of China (No.20473078) and the Specialized Research Fund for the Doctoral Program of Higher Education (No.200803580022).

DOI:10.1088/1674-0068/22/04/346-352

[1] R. M. Pearlstein, *in Photosynthesis*, J. Amesz, Ed., Amsterdam: Elsevier, 299 (1987).
[2] G. McDermott, S. M. Prince, A. A. Freer, A. M. Hawthornthwaite-Lawless, M. Z. Papiz, R. J. Cogdell, and N. W. Isaacs, Nature **374**, 517 (1995).
[3] F. C. Spano and S. Mukamel, Phys. Rev. A **40**, 5783 (1989).
[4] Y. Kureishi, H. Shiraishi, and H. Tamiaki, J. Electroanal. Chem. **496**, 13 (2001).
[5] D. J. Fermin, H. D. Duong, Z. Ding, P. F. Brevet, and H. H. Girault, J. Am. Soc. Chem. **121**, 10203 (1999).
[6] T. H. Tran-Thi, J. F. Lipskier, D. Houde, C. Pepin, E. Keszei, and J. P. Jay-Gerin, J. Chem. Soc. Faraday Trans. **88**, 2129 (1992).
[7] R. F. Pasternack, K. F. Schaefer, and P. Hambright, Inorg. Chem. **33**, 2062 (1994).
[8] O. Ohno, Y. Kaizu, and H. Kobayashi, J. Chem. Phys. **99**, 4128 (1993).
[9] G. A. Schick, M. R. O'Grady, and R. K. Tiwari, J. Phys. Chem. **97**, 1339 (1993).
[10] J. M. Ribo, J. Crusats, J. A. Farrera, and M. L. Valero, J. Chem. Soc. Chem. Commun. 681 (1994).
[11] J. M. Ribo, J. Crusats, F. Sagues, J. Claret, and R. Rubires, Science **292**, 2063 (2001).
[12] R. Rotomskis, R. Augulis, V. Snitka, R. Valiokas, and B. Liedberg, J. Phys. Chem. B **108**, 2833 (2004).
[13] D. L. Akins, H. R. Zhu, and C. Guo, J. Phys. Chem. **100**, 5420 (1996).
[14] D. L. Akins, S. Ozcelik, H. R. Zhu, and C. Guo, J. Phys. Chem. **100**, 14390 (1996).
[15] D. L. Akins, S. Ozcelik, H. R. Zhu, and C. Guo, J. Phys. Chem. A **101**, 3251 (1997).
[16] D. M. Chen, T. J. He, D. F. Cong, Y. H. Zhang, and F. C. Liu, J. Phys. Chem. A **105**, 3981 (2001).
[17] Y. H. Zhang, D. M. Chen, T. J. He, and F. C. Liu, Spectrochim. Acta A **59**, 87 (2003).
[18] D. M. Chen, Y. H. Zhang, T. J. He, and F. C. Liu, Spectrochim. Acta A **58**, 2291 (2002).
[19] M. Y. Choi, J. A. Pollard, M. A. Webb, and J. L. McHale, J. Am. Chem. Soc. **125**, 810 (2003).
[20] S. C. Doan, S. Shanmugham, D. E. Aston, and J. L. McHale, J. Am. Chem. Soc. **127**, 5885 (2005).
[21] L. M. Scolaro, A. Romeo, M. A. Castriciano, G. D. Luca, S. Patane, and N. Micali, J. Am. Chem. Soc. **125**, 2040 (2003).
[22] G. D. Luca, A. Romeo, and L. M. Scolaro, J. Phys. Chem. B **109**, 7149 (2005).
[23] A. Mammana, A. D'Urso, R. Lauceri, and R. Purrello, J. Am. Chem. Soc. **129**, 8062 (2007).
[24] T. Nagahara, K. Kisoda, H. Harima, M. Aida, and T. A. Ishibashi, J. Phys. Chem. B **113**, 5098 (2009).
[25] L. C. Xu, Z. Y. Li, W. Tan, T. J. He, F. C. Liu, and D. M. Chen, Spectrochim. Acta A **62**, 850 (2005).
[26] X. Y. Li, R. S. Czernuszewicz, J. R. Kincaid, Y. O. Su, and T. G. Spiro, J. Phys. Chem. **94**, 31 (1990).
[27] T. S. Rush III, P. M. Kozlowski, C. A. Piffat, R. Kumble, M. Z. Zgierski, and T. G. Spiro, J. Phys. Chem. B **104**, 5020 (2000).
[28] M. Gouterman, *In Porphyrins*, D. Dolphin, Ed., Vol. 3, New York: Academic Press, 1 (1978).
[29] R. F. Pasternack, C. Bustamante, P. J. Collings, A. Giannetto, and E. Gibbs, J. Am. Chem. Soc. **115**, 5393 (1993).
[30] R. F. Pasternack and P. J. Collings, Science **269**, 935 (1995).
[31] G. Arena, L. M. Scolaro, R. F. Pasternack, and R. Romeo, Inorg. Chem. **34**, 2994 (1995).
[32] J. C. de Paula, J. H. Robblee, and R. F. Pasternack, Biophys. J. **68**, 335 (1995).
[33] T. G. Spiro and X. Y. Li, *In Biological Application of Raman Spectroscopy*, Vol.3, T. G. Spiro, Ed., New York: Wiley-Interscience, 1 (1988).
[34] Q. S. Mortensen and S. Hassing, Adv. IR & Raman Spectrosc. **6**, 1 (1980).
[35] X. Z. Song, W. Jentzen, S. L. Jia, L. Jaquinod, D. J. Nurco, C. J. Medforth, K. M. Smith, and J. A. Shelnutt, J. Am. Chem. Soc. **118**, 12975 (1996).

DOI:10.1088/1674-0068/22/04/346-352